Int. J. Heat Mass Transfer. Vol. 18, pp. 1377–1386. Pergamon Press 1975. Printed in Great Britain

COMBUSTION AND FLAME SPREADING PHENOMENA IN GAS-PERMEABLE EXPLOSIVE MATERIALS

W. F. VAN TASSELL and H. KRIER
Aeronautical and Astronautical Engineering Department,
University of Illinois at Urbana-Champaign, IL 61801, U.S.A.

(*Received* 29 *May* 1974 *and in revised form* 24 *February* 1975)

Abstract—Combustion and flame spreading in gas-permeable beds of solid propellant grains are analyzed in this paper. A theoretical model based on continuum mechanics concepts is first formulated. The Lax–Wendroff finite difference technique is then used to generate some numerical solutions. The sensitivity of the model to propellant characteristics, heat transfer and drag correlations, and propellant bed packing density is established by the numerical results. It is concluded that propellant properties, particularly the energy release rate and the burning rate index, are the most critical parameters in this problem. The lack of adequate heat transfer and drag correlations for reactive flows is also noted.

NOMENCLATURE

b_1, b_2, burning rate constants, $\dot{r} = b_1 + b_2 p^n$;
B_s, drag parameter, see equation (26);
C^α, species mass fraction;
$\hat{C}^\alpha$, species mass source term;
C_p, mixture specific heat at constant pressure;
C_p^α, species specific heat at constant volume;
C_v^α, species specific heat at constant volume;
$\mathscr{D}$, drag term as written in equation (26);
D_p, particle reference diameter;
e^α, specific internal energy of species α;
$\hat{e}_\alpha$, energy source term;
e, mixture internal energy;
E, mixture total energy;
E^α, species total energy;
E^α_{chem}, energy release rate;
f_i, mixture body force;
f_i^α, species body force;
h_i, mixture energy flux term;
h_i^α, species energy flux term;
h, heat-transfer coefficient;
n, burning rate index;
P, mixture pressure;
p^α, species partial pressure;
$\hat{p}_i^\alpha$, species momentum source;
Pr, Prandtl number, $\mu C_p/k$;
Q^α, species body heating;
Q, mixture body heating;
$\mathscr{R}$, denotes number of species;
R_p, propellant grain radius;
Re_p, Reynolds number;
$\dot{r}$, burning rate;
T, mixture temperature;
T^α, temperature of species α;
t, time;
U_i, mixture velocity;
$\mathscr{U}_i^\alpha$, diffusion velocity of species α;
v_i^α, velocity of species α;
x, coordinate along propellant bed;
x_i^α, position of species α;
$\ddot{x}_i^\alpha$, defined by $\dfrac{\partial v_i^\alpha}{\partial t} + v_j^\alpha \dfrac{\partial v_i^\alpha}{\partial x_j}$.

Greek symbols

α, denotes a species;
Γ^α, mass source term, equation (51);
κ, mixture thermal conductivity;
ρ, density;
ρ^α, density of species α;
τ_{ij}, mixture stress tensor;
τ_{ij}^α, species stress tensor;
ϕ, void fraction = gas volume/total volume.

1. INTRODUCTION

COMBUSTION and flame spreading phenomena in gas–permeable explosive systems, such as packed beds of solid propellant grains, have recently been the subject of experimental and theoretical work. The propellant grains are ignited in an accelerated manner and pressure and velocity gradients are established, eventually resulting in wave propagations throughout the porous medium, if the total volume of the system is allowed to increase. As a result of the penetration of the hot combustion products from a propagating flame front into the porous material, heat transfer by conduction is essentially replaced by convective transfer.

An adequate understanding of these problems requires constructing a two-phase flow model which includes the effects of heat, mass, and momentum transfer. Results obtained with such an analytical model are presented herein. A schematic, indicating some important features of the problem, is shown on Fig. 1.

The phenomena associated with flame spreading and combustion in porous propellant beds may be described as follows. At some initial instant the propellant in a portion of the bed is ignited. The combustion gases flow through the porous propellant bed, igniting more propellant and generating greater quantities of gas. The entire process accelerates until shot start time. After shot start, rarefaction waves propagate back into the propellant bed. The increasing volume now allows substantial movement of the propellant particles to take place. The entire process continues until the chamber is evacuated to atmosphere or until all the propellant is burned.

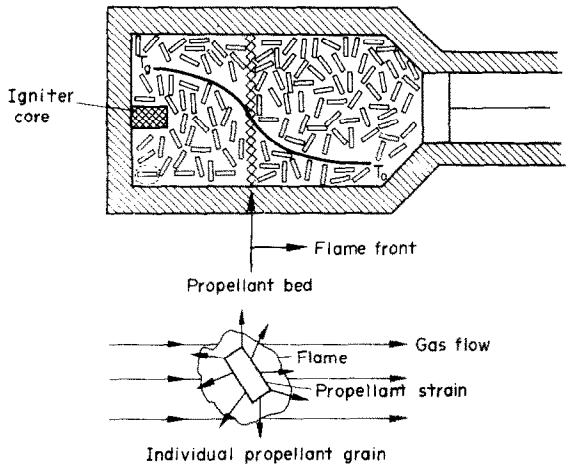

FIG. 1. Propellant grain bed with propagating convective flame front.

The complexity of this problem is self evident, and it is only recently that the analysis of this process has been undertaken. The dissertation by Kuo [1] (see also [2, 3]) represents the first reported analytical results in this area. Several organizations and government agencies are now engaged in research on this problem. A comparison and review of some of these studies was presented in [4].

With any problem this complex, a uniform and universally agreed upon theoretical formulation can not be expected. At least three different theoretical approaches have been proposed for problems such as this. These three approaches might descriptively be called (1) statistical theory, (2) averaging theory, and (3) continuum mechanics theory. The statistical theory has not been applied to this combustion problem. Several possible statistical approaches are outlined in Beran's text [5]. The most comprehensive studies to date are those of Buyevich [6–8]. These studies have not been generalized to include reacting flows, and hence, it is not possible to judge the usefulness of this approach.

The theory of averaging assumes that the flow behavior can be determined from a model consisting of a combusting solid propellant suspended in a Navier–Stokes fluid. The governing equations are derived by averaging the various flow properties over regions large compared with the particle size, but small compared with the macroscopic scale of the apparatus. Among the better known theories are those of Anderson and Jackson [9] and Whitaker [10].

Gough and Zwarts [11] have generalized the Anderson and Jackson theory for this problem. Some results for closed chamber burning are given in their report. The results appear reasonable, although the amount of empirical data required by this problem is extensive. Gough and Zwarts [12] are also applying the Whitaker techniques, but this work is not complete at this time. The various averaging techniques appear to offer a reasonable approach to this problem. It is too early to tell if this is the "best" approach.

2. FORMULATION OF THEORETICAL MODEL

This particular research is based on the earlier studies of Kuo, Vichnevetsky and Summerfield [2]. The original Kuo theory assumed a packed bed and a closed volume. The research reported herein was motivated by the necessity of providing calculations applicable to a highly mobile propellant bed subjected to large volume changes. From this consideration, it was evident that the Kuo theory was not adequate as originally presented. Fisher and Trippe [13] modified the Kuo–Summerfield analysis to presumably allow for propellant motion. This model was then used to investigate some specific gun gystems. A similar approach was also used in the more recent model developed by East and McClure [14]. All of these models, either implicitly or explicitly, are based on the concepts of continuum mechanics.

The basic species balance equations were derived in detail by Truesdell [15, 16]. The derivations will not be repeated here. Rather, the species balance equations will simply be written down. This will be followed by a discussion of the particular constitutive assumptions used in our model. It is understood that each identifiable component of the multiphase flow requires a separate species balance equation. In subsequent sections, this analysis will be restricted to two species; a gas species and a solid (propellant) species. Any further generalizations are not warranted at this time.

The species balance equations are:

$$\frac{\partial \rho^\alpha}{\partial t}+\frac{\partial}{\partial x_i}(\rho^\alpha v_i^\alpha)=\rho\hat{C}^\alpha \tag{1}$$

$$\rho^\alpha\hat{C}^\alpha v_i^\alpha+\rho^\alpha(\ddot{x}_i^\alpha-f_i^\alpha)-\frac{\partial}{\partial x_j}(\tau_{ij}^\alpha)=\rho\hat{p}_i^\alpha \tag{2}$$

where $\tau_{ij}^\alpha=\tau_{ji}^\alpha$, is assumed.

$$\rho\hat{e}^\alpha=\rho\hat{p}_i^\alpha v_i^\alpha+\rho\hat{C}^\alpha\left[e^\alpha-\tfrac{1}{2}v_i^\alpha v_i^\alpha\right]+\rho\dot{e}^\alpha - \tau_{ij}^\alpha\frac{\partial v_j^\alpha}{\partial x_i}-\frac{\partial h_i^\alpha}{\partial x_i}-\rho^\alpha Q^\alpha \tag{3}$$

where $$\dot{e}^\alpha\equiv\frac{\partial e^\alpha}{\partial t}+v_i^\alpha\frac{\partial e^\alpha}{\partial x_i}.$$

The mixture variables are related to the corresponding species variables by the following:

$$\rho=\sum_{\alpha=1}^{\mathscr{N}}\rho^\alpha \tag{4a}$$

$$\rho U_i=\sum_{\alpha=1}^{\mathscr{N}}\rho^\alpha v_i^\alpha \tag{4b}$$

$$\tau_{ij}=\sum_{\alpha=1}^{\mathscr{N}}\{\tau_{ij}^\alpha-\rho^\alpha\mathscr{U}_i^\alpha\mathscr{U}_j^\alpha\} \tag{4c}$$

$$f_i=\sum_{\alpha=1}^{\mathscr{N}}C^\alpha f_i^\alpha \tag{4d}$$

$$\rho e=\sum_{\alpha=1}^{\mathscr{N}}\rho^\alpha(e^\alpha+\tfrac{1}{2}\mathscr{U}_i^\alpha\mathscr{U}_i^\alpha) \tag{4e}$$

$$Q=\sum_{\alpha=1}^{\mathscr{N}}C^\alpha(Q_I^\alpha+f_i^\alpha\mathscr{U}_i^\alpha) \tag{4f}$$

$$h_i=\sum_{\alpha=1}^{\mathscr{N}}\left[h_i^\alpha+\tau_{ij}^\alpha\mathscr{U}_j^\alpha-\rho^\alpha(e^\alpha+\tfrac{1}{2}\mathscr{U}_i^\alpha\mathscr{U}_i^\alpha)\mathscr{U}_i^\alpha\right]. \tag{4g}$$

In the above equations $\hat{C}^\alpha$, $\hat{p}_i^\alpha$, and $\hat{e}^\alpha$ are the mass momentum, and energy source terms for species α; τ_{ij}^α is the species partial stress and h_i^α the species partial heat flux; Q is the body heating and $\mathscr{U}_i^\alpha$ is the species diffusion velocity, defined by

$$\mathscr{U}_i^\alpha = v_i^\alpha - U_i.$$

The barycentric velocity, U_i, is defined by equation (4b).

The above balance equations contain the mechanical aspects of a multiphase mixture theory. The various continuum mechanics models are distinguished by the thermodynamic assumptions used. The general theory of constituitive relations is complicated, and has not been developed for this problem. In this sense, all of the continuum mechanics models are ad hoc. The details of constructing a constituitive theory have been presented by Kelly [17] and Truesdell [16], among others.

Constituitive relations are required for the source terms ($\hat{C}^\alpha$, $\hat{P}_i^\alpha$), the species partial stress and internal energy (τ_{ij}^α, e^α), and the heat fluxes (h_i^α, Q_i^α). No general studies on formulating appropriate constituitive relations for this problem have been reported. The current practice is to treat each variable separately. A unified theory for this problem must wait until the necessary theoretical thermodynamics formalism is complete.

The present model used the approach given by Soo [18]. This is supplemented by a more specific formulation of the source terms. The details may be found in [4].

The mass source term is written as

$$\rho\hat{C}^\alpha = \Gamma^\alpha \tag{5}$$

where for an isolated burning spherical particle

$$\Gamma^g = \frac{3(1-\phi)}{R_p}\rho_p \dot{r} \tag{6}$$

and

$$\Gamma^p = -\Gamma^g$$

ρ_p = propellant density, assumed constant

R_p = propellant particle radius

$\dot{r}$ = propellant burning rate

ϕ is the void fraction, and is defined as the ratio of the gas volume to the total system volume. Note

$$\rho^g = \frac{M^g}{v^T} = \frac{M^g}{v^g}\frac{v^g}{v^T} = \rho_g\phi$$

where ρ_g is the usual gas density based on the gas volume. Similarly

$$\rho^p = (1-\phi)\rho_p$$

where ρ_p is the density of the propellant particle. For our calculations we take

$$\dot{r} = b_1 + b_2(P_g)^n \tag{7}$$

where b_1, b_2 and n are constants. Subscripts p and g refer to the propellant and gas respectively. Equation (6) can also be derived for isolated particles of other geometries. However, it is more in keeping with a continuum theory to simply take $\Gamma = A\dot{r}$ and to recognize that A will change for different propellant configurations.

Turning to the momentum equation, we choose to write the source term as

$$\hat{p}_i^\alpha - \mathscr{U}_i^\alpha\rho\hat{C}^\alpha \equiv \hat{p}_i^\alpha - \Gamma^\alpha\mathscr{U}_i^\alpha.$$

The important fact to remember is that this combination of terms must account for *all* of the interactions between the gas and solid species. As formulated above, we must have

$$\sum_{\alpha=1}^{\mathscr{N}} \hat{p}_i^\alpha \equiv 0.$$

Hence, $\hat{p}_i$ is interpreted as the force on the gas, while $\hat{p}_i^p = -\hat{p}_i^g$ would be the force on the propellant. This force will be determined by a semi-empirical correlation. The remaining term, which arises simply from the formal manipulations, can be interpreted as the momentum decrement due to the differences in velocity between the gas and solid phases.

The species stress tensor is assumed to be the thermodynamic pressure, plus an apparent stress due to diffusion.

$$\tau_{ij}^g = -p^g\delta_{ij} + \rho^g\mathscr{U}_i^g\mathscr{U}_j^g. \tag{8}$$

Note the effect of molecular transport has been deleted (no viscosity). The solid particles are relatively massive, and it is assumed that no random thermal motions occur. In effect, we assume

$$\tau_{ij}^p \equiv 0 + \rho^p\mathscr{U}_i^p\mathscr{U}_j^p. \tag{9}$$

The species energy equation is given by Soo [18] in terms of the total energy per unit mass

$$E^\alpha = e^\alpha + \tfrac{1}{2}v_i^\alpha v_i^\alpha \tag{10}$$

where e^α is the specific internal energy. The balance equation, in this variable, becomes

$$\rho^\alpha\left[\frac{\partial E^\alpha}{\partial t} + v_i^\alpha\frac{\partial E}{\partial x_i}\right] = \left[\frac{\partial}{\partial x_j}v_i^\alpha\tau_{ij}^\alpha\right] - \Gamma^\alpha E^\alpha + \frac{\partial}{\partial x_j}(h_j^\alpha) + Q_I^\alpha + \rho\hat{e}^\alpha. \tag{11}$$

The term corresponding to the momentum source term in the energy equation does not appear when the total energy, E^α, is used as a variable. The energy source term, $\rho\hat{e}^\alpha$, contains two parts, and can be written as

$$\rho\hat{e}^\alpha = C_p^\alpha\rho^\alpha\sum_{\substack{\alpha=1\\ \alpha\neq 1}}^{\mathscr{N}} G^{\beta\alpha}(T^\alpha - T^\beta) + \Gamma^\alpha E_{\text{Chem}}^\alpha. \tag{12}$$

The first accounts for the exchange of heat by conduction between the species. In this case, this is interpreted to be the heat transferred to the solid. Since this is viewed as an interchange, we require

$$\sum_\alpha\sum_\beta C_p^\alpha\rho^\alpha G^{\beta\alpha}(T^\alpha - T^\beta) = 0. \tag{13}$$

The chemical source term, $\Gamma^\alpha E_{\text{Chem}}^\alpha$, arises only if the heats of formation are not included in the definition of E^α. This has been assumed to be the case here, i.e.

$$E^\alpha \equiv \int_{T_0}^{T} C_v^\alpha\,\mathrm{d}T + \tfrac{1}{2}(v_i)^2. \tag{14}$$

The heat flux vector is written as

$$h_j^\alpha = \kappa\left\{\frac{\rho^\alpha C_p^\alpha}{\rho C_p}\frac{\partial T}{\partial x_j} + T^\alpha\frac{\partial}{\partial x_j}\left(\frac{\rho^\alpha C_p^\alpha}{\rho C_p}\right) + \frac{\partial}{\partial x_j}\left(\frac{v_i^\alpha \rho^\alpha \mathscr{U}_i^\alpha}{2\rho C_p}\right)\right\} + \rho^\alpha \mathscr{U}_i^\alpha E^\alpha. \quad (15)$$

Consistent with setting the viscosity to zero, we now set κ to zero. In this case, then, the heat flux is due solely to the diffusion of E^α. Note that in changing variables, the stress work term has been written as a separate quantity.

Finally, the body heating term is given by

$$Q_I = \frac{\rho^\alpha C_p^\alpha}{\rho C_p} Q^* - \frac{\partial}{\partial x_j}\{\mathscr{U}_i^\alpha \tau_{ij}^\alpha\} \quad (16)$$

where dissipation due to relative motion has been included. Q^* is the externally supplied heat flux.

For a two phase, solid–gas mixture, some more thermodynamic assumptions can be made. First, recall that the solid phase thermodynamic pressure was taken to be zero. We now assume that the gas phase thermodynamic variables can be related by a state equation of the form

$$P_g = P_g(\rho_g, T_g).$$

The perfect gas law was used for initial calculations.

To complete this section, the governing species balance equations will be written for the one dimensional, unsteady flow situation. The void fraction is used as an explicit variable. With this in mind, the balance equations assume the following form:

Mass balances

Gas phase

$$\frac{\partial}{\partial t}(\phi\rho_g) + \frac{\partial}{\partial x}(\phi\rho_g v_g) = \Gamma_g \quad (17)$$

Solid phase

$$\frac{\partial}{\partial t}[(1-\phi)\rho_p] + \frac{\partial}{\partial x}[(1-\phi)\rho_p v_p] = \Gamma_p. \quad (18)$$

Momentum balances

Gas phase

$$\rho_g\phi\left[\frac{\partial v_g}{\partial t} + v_g\frac{\partial v_g}{\partial x}\right] = -\frac{\partial}{\partial x}(\phi P_g) + \frac{\partial}{\partial x}[\rho_g\phi(v_g-U)^2] - (v_g-U)\Gamma^g + \mathscr{D} \quad (19)$$

Solid phase

$$(1-\phi)\rho_p\left[\frac{\partial v_p}{\partial t} + v_p\frac{\partial v_p}{\partial x}\right] = \frac{\partial}{\partial x}[(1-\phi)\rho_p(v_p-U)^2] - (v_p-U)\Gamma^p - \mathscr{D} \quad (20)$$

where

$$\rho_p(1-\phi)v_p + \rho_g\phi v_g = \rho U \quad (21)$$

and

$$(1-\phi)\rho_p + \phi\rho_g = \rho. \quad (22)$$

Energy balances

Gas phase

$$\phi\rho_g\left[\frac{\partial E_g}{\partial t} + v_g\frac{\partial E_g}{\partial x}\right] = \frac{\partial}{\partial x}\{v_g[-\phi\rho_g + \rho_g\phi\mathscr{U}_g^2]\} - \Gamma^g(E_g - E_{\text{chem}}^g) + \frac{\partial}{\partial x}[\phi\rho_g\mathscr{U}_g E_g] - \frac{\partial}{\partial x}\{\mathscr{U}_g[-\phi p_g + \rho_g\phi\mathscr{U}_g^2]\} + \frac{-3(1-\phi)}{r_p}\bar{h}(T_g - T_p) \quad (23)$$

Solid phase

$$(1-\phi)\rho_p\left[\frac{\partial E_p}{\partial t} + v_p\frac{\partial E_p}{\partial x}\right] = \frac{\partial}{\partial x}\{v_p[(1-\phi)\rho_p\mathscr{U}_p^2]\} - \Gamma^p(E_p - E_{\text{chem}}^p) + \frac{\partial}{\partial x}[(1-\phi)\rho_p E_p\mathscr{U}_p] - \frac{\partial}{\partial x}\{\mathscr{U}_p[(1-\phi)\rho_p\mathscr{U}_p^2]\} + 3\frac{(1-\phi)}{r_p}\bar{h}(T_g - T_p). \quad (24)$$

Initial and boundary conditions are required by this formulation. The initial values of all flow variables are assumed to correspond to some nominal ambient condition (one atmosphere of pressure and a temperature of 540°R). At the initial instant, the primer introduces hot gases over a certain length of the propellant bed. The action of the primer gases upon the propellant is itself a difficult problem. We have chosen to model the primer as a simple mass source, specified as a function of x and t. The primer gases do not compact the propellant bed. Because a one dimensional model is being used, instantaneous mixing in the radial direction is assumed.

For these initial calculations, no heat-transfer losses are assumed to occur. In addition, no mass is allowed to cross the boundaries of the computational field. Numerically, these boundary conditions are expressed by a standard reflection technique.

Calculations require a knowledge of all of the source terms present. Since no relevant body of experimental data or theory is available, these source terms will have to be formulated on an ad hoc basis. Hence, a semi-empirical data base is part of this problem and introduces some more uncertainty.

The data required include the following: (1) an ignition model, (2) a burning rate correlation, (3) a drag correlation, (4) a heat transfer correlation, and (5) an energy release rate. These data will be discussed briefly here.

In [11], some current ignition models are discussed. The present model employs the simplest ignition model possible. Namely, if the particle bulk temperature exceeds 570°R, the propellant is said to be ignited. This ignition temperature was chosen to correspond to a 30°R rise over the initial ambient bulk temperature. In [4], some simple procedures for relating the bulk temperature to the propellant surface temperature are

given. This will allow the use of other ignition criteria, should the need arise.

The burning rate law was taken to be of the form

$$\dot{r} = b_1 + b_2 p^n. \tag{25}$$

The nominal case used the following values.

$$n = 2/3$$
$$b_1 = 0{\cdot}0303 \text{ in/s}$$
$$b_2 = 0{\cdot}00253 \text{ in/s (lb/in}^2)^n.$$

The drag correlation used was based on the formula proposed by Ergun [19]. The Ergun relation is

$$\mathscr{D} = \rho_g \frac{(v_g - v_p)|v_g - v_p|}{D_p}(1-\phi)\left\{\frac{150(1-\phi)}{\phi Re_p} + B_s\right\} \tag{26}$$

where $B_s = 1{\cdot}75$. Our results indicate that the Reynolds number term can be omitted, and that a good value for B_s is 0·175. Note that

$$D_p = \frac{6 \text{ (volume of particle)}}{\text{surface area of particle}}$$

$$Re_p = g^{\frac{D_p|v_g - v_p|}{\mu g}}.$$

The heat-transfer correlation comes from fluidized bed data and was proposed by Gelperin and Einstein [20]. This correlation is used without change. The film heat-transfer coefficient is given by

$$h = \frac{k_g}{D_p}\{2 + ARe_p^{2/3}Pr^{1/3}\} \tag{27}$$

where

$$A = 0{\cdot}4.$$

The energy release rates used are typical values for gun propellant. The heat of combustion was assumed to be 1000 cal/g while the heat of vaporization was taken to be 100 cal/g. These values can be measured experimentally for any gun propellant of interest.

A geometry of the grain must be specified so that the instantaneous burning surface area can be calculated. Typically a multi-perforated cylindrical shape is used; the webb dimensions are given in Table 1.

The drag and heat-transfer correlations represent one of the important unknowns in this problem. Many of the available data correlations are for the low speed flow of a gas through a packed bed of glass spheres. In the present problem the flow in the propellant undergoes transition from the packed bed regime to the fluidized bed regime, and then into a pneumatic transport regime. Throughout this process, the particles are burning. Ideally one would like a single data correlation that would describe the totality of flow regimes.

Because of the lack of good data, the simple data correlations discussed above were used. A more complete discussion of the heat-transfer and drag data available is presented in [4].

3. DISCUSSION OF RESULTS

In this section a variety of numerical results will be presented and discussed. As mentioned previously, many of the parameters occurring in this problem are not known. Hence, the majority of the results were generated in order to examine the sensitivity of the numerical solution to the input parameters. By doing this, we hope to establish which parameters are most critical.

The equations developed in Section 2 were solved by a finite-difference numerical technique. In particular, the Richtmyer two step variation of the Lax–Wendroff scheme was used. This scheme is conditionally stable, contingent upon satisfying the Courant–Friedricks–Lewy condition. An explicit artificial viscosity was introduced in order to provide diffusive damping and to ensure stability in the presence of strong source terms. Complete details are given in [4] or the standard texts on numerical analysis.

The results given in this section are all based on a standard case. On most figures, the standard case will be compared with results corresponding to the variation of a single input parameter. The standard case input values are listed in Table 1.

On Fig. 2, the effects of varying the drag correlation in the propellant bed are shown. The curve labeled B_s is the standard case, while the curve labeled $10B_s$ corresponds approximately to the Ergun drag correlation, and so on. Note that as the drag increases, the pressures in the bed become more uniform, and a smaller percentage of the propellant is ignited at shot

Table 1. Standard case input values and definitions

Parameter	Value	Units	Definition
ϕ_0	0·44	—	Initial void fraction in propellant bed
T_0	540	°R	Initial temperature of gas and propellant
n	2/3	—	Burning rate pressure index
b_1	0·0303	in/s	Burning rate constant
b_2	0·00253	in/s (lb/in^2)^n	Burning rate pre-exponential factor
L^*	30	in	Length of propellant bed
T_{p_i}	590	°R	Bulk ignition temperature of propellant
E_{chem}	$1{\cdot}15 \times 10^3$	cal/g	Energy release rate during combustion
A	0·4	—	Heat-transfer constant
B_s	0·175	—	Drag correlation constant
W	0·025	in	Initial perforation diameter
D	0·25	in	Grain outside diameter
L	0·50	in	Grain length

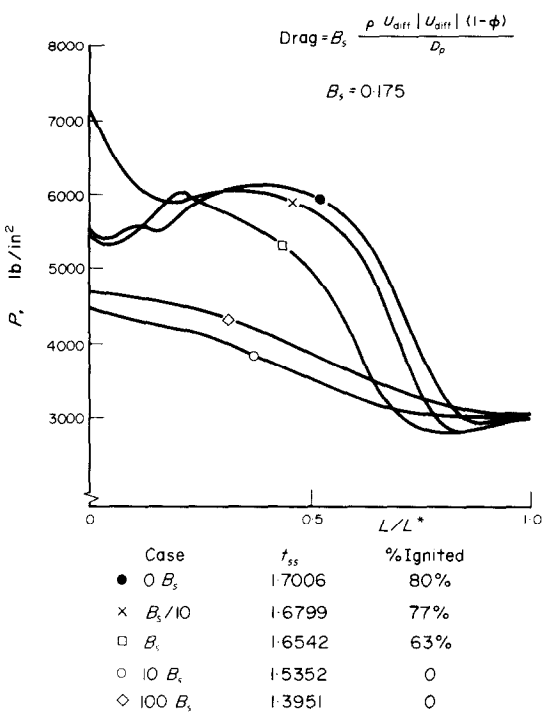

FIG. 2. Pressure distribution at shot-start conditions: the effect of the gas-particle drag parameter.

start. At the highest drag calculated, none of the bed was ignited. With high drag the gas velocity will be low, and the rate of convective heat transfer will be low. The primer gas simply pressurized the propellant bed. At some point the shot start pressure, here assumed to be 3000 lb/in^2, was reached and the calculations were stopped. As can be seen, the drag can vary over a wide range. While the behavior of the propellant bed is sensitive to the drag, there is nothing in these results that would indicate any catastrophic results if the propellant grain were "high drag" or "low drag".

A similar conclusion can be reached when the heat transfer correlation is examined. As shown on Fig. 3, the pressure distributions at shot start are relatively insensitive to the heat-transfer correlations. As expected, as the heat-transfer coefficient increases, more of the bed is ignited and more gas is generated near the breech end of the bed. The subsequent pressure gradient drives a larger axial mass flow toward the projectile base, and this process tends to equilibrate the pressure distribution. Again, aside from a fluid mechanical interest, the heat-transfer correlation does not appear to be a sensitive parameter.

Figures 4 and 5 show the sensitivity of the shot start pressure distributions to the propellant energy release rate and the burning rate index. As would be expected, the physical properties and burning rate of the propellant are very important and are among the most sensitive of all parameters. Figure 4 shows the effect of varying the energy release rate. The results shown on Fig. 4 reflect the usual situation. Here a 20 per cent change in energy release rate leads to about a 10 per cent change in peak pressure. Order of magnitude changes were required in drag in order to have the same effect.

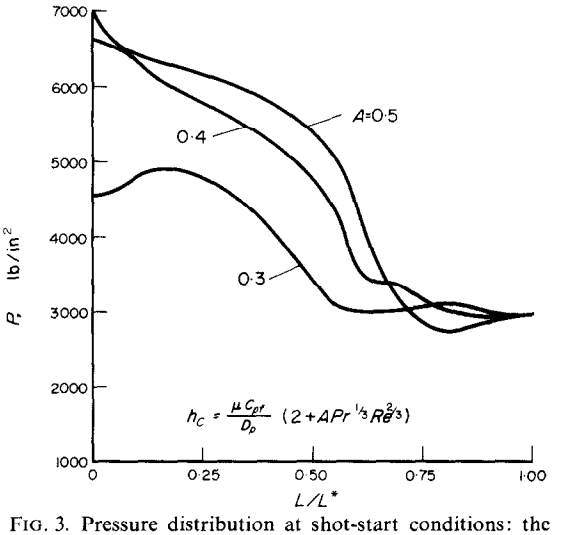

FIG. 3. Pressure distribution at shot-start conditions: the effect of the gas-particle heat-transfer parameter.

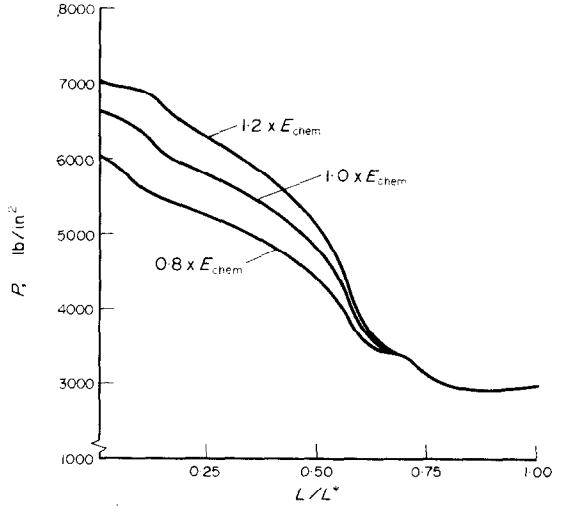

FIG. 4. Pressure distribution at shot-start conditions: the effect of propellant energy release rate.

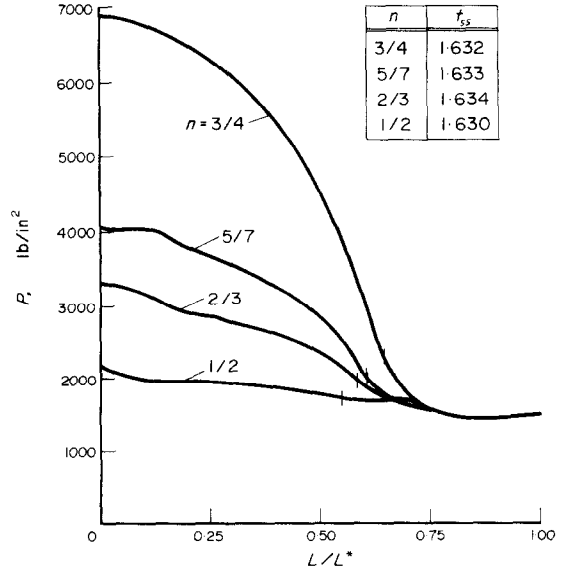

FIG. 5. Pressure distribution at shot-start conditions: the variations in burning rate-pressure index.

Hence, this is a sensitive parameter. Fortunately, it is usually carefully measured.

On Fig. 5 the effects of varying the burning rate index are shown. The vertical bars indicate the flame front position at shot start. As can be seen from the values given, shot start times are relatively insensitive to the burning rate index. However, peak pressures are extremely sensitive, varying by a factor of three as the pressure index, n, increases from 1/2 to 3/4. For accurate results, this parameter must be known precisely. It is also evident that a theoretician could match any given pressure level simply by adjusting the burning rate index. Hence, any "agreement" between theory and experiment must be examined in great detail.

The effects of varying the initial packing density, or porosity, are shown on Fig. 6. Recall smaller values

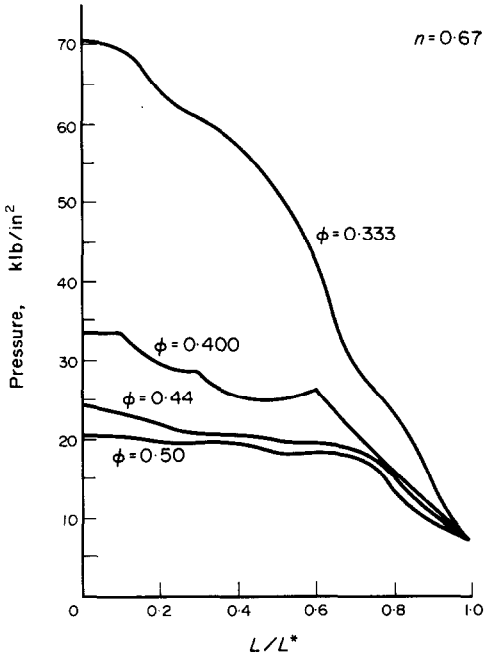

FIG. 6. Pressure distribution at shot-start conditions: the effect of initial void fraction.

of ϕ indicate greater solid loadings. The pressure profiles shown at a time when the rear face has reached a pressure of 7000 lb/in^2. The time to reach this pressure is different for each, and more of the bed is ignited as ϕ decreases.

It should be emphasized here that the model has specifically assumed no particle–particle interaction. As ϕ is lowered to values of 0·30, a packed bed condition is reached. In a packed bed, however, the collision of the propellant grains will be an important factor in determining the pressure distribution. The proper analysis for the particle stress tensor at these conditions will require further research and complementary experiments at these high pressure-unsteady flow regimes.

The present model carefully defines several velocity variables. Figure 6 gives the velocity distributions at 1·97 ms for a moderately loaded bed. Note the flow reversal for both the gas and the solid grains at the first 20 per cent of the bed at this instance. This result emphasizes the need for being careful in defining and calculating all velocities.

A composite gas velocity, temperature and pressure distribution at shot-start conditions are shown in Fig. 8 for $\phi = 0{\cdot}40$. Here the igniter stub was reduced to 1/2 its typical length. The peak pressure is predicted to occur in the interior of the bed, producing a "continental divide" as discussed by Kuo *et al.* [2]. On

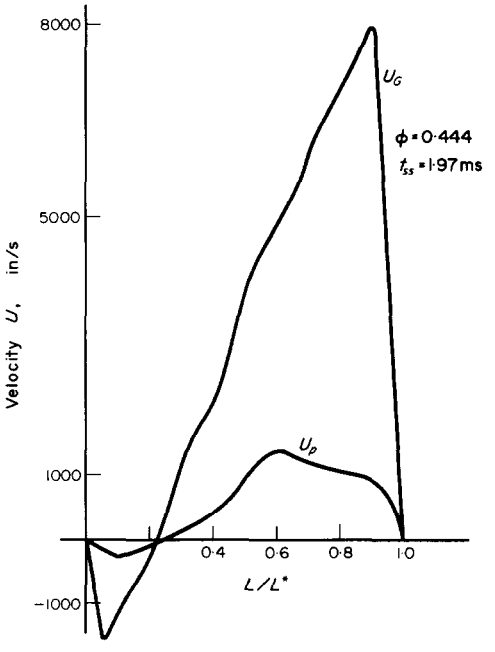

FIG. 7. Gas and particle velocity distribution at shot-start conditions.

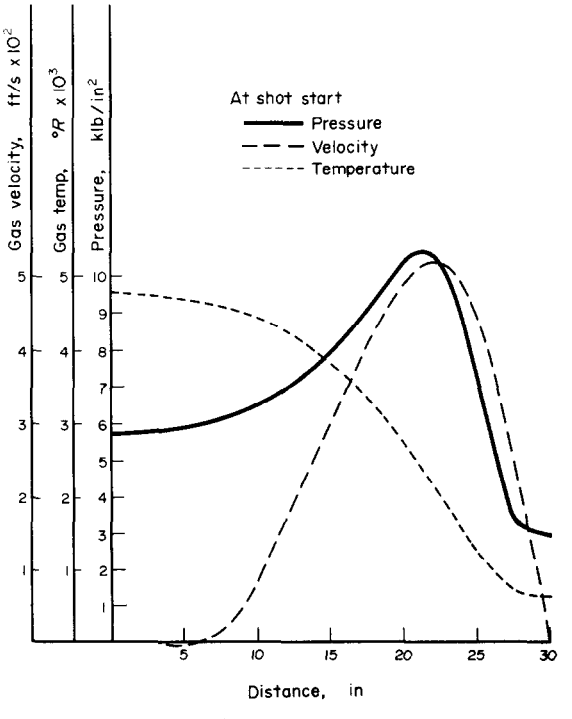

FIG. 8. Pressure, velocity and temperature distribution at shot-start: short igniter conditions.

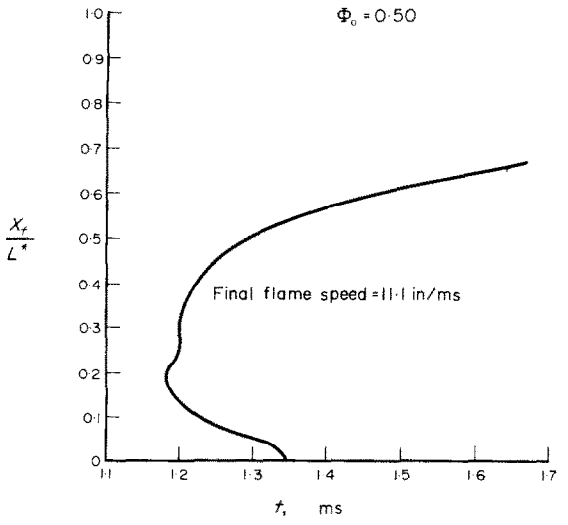

FIG. 9. Locus of points of the ignition front (flame).

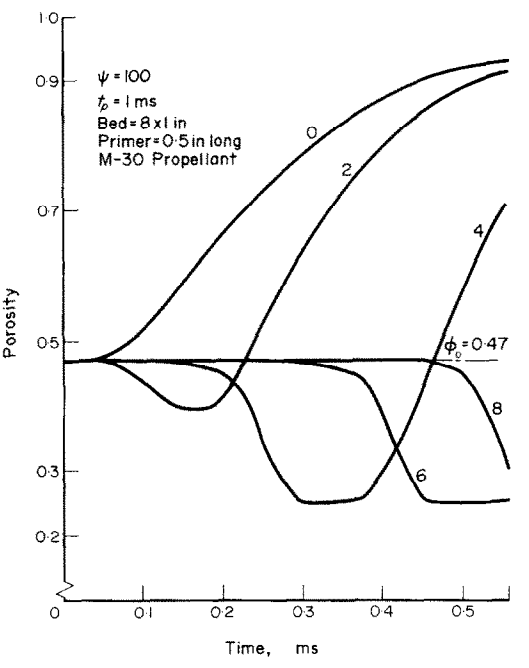

FIG. 10. Propellant bed porosity vs time at four positions in an 8·0 in long bed.

Fig. 9 the calculated ignition front (or flame front) location is shown as a function of time. As can be seen, at about 1·2 ms, ignition first occurs. Note that the initial flame location is about 20 per cent of the length from the breech end of the propellant bed. This initial flame location is strongly dependent upon the assumed form of the primer function. After the initial ignition event, the flame spreads in both directions. At about 1·35 ms the flame reaches the breech end of the bed. About half of the propellant is ignited by this time. At later times, the flame continues to spread into the unburned propellant. An asymptotic flame speed of about 11·1 in/ms is indicated when the shot start pressure of 3000 lb/in^2 is reached. Roughly 70 per cent of the bed is ignited at this point.

Because of the solid grain motion, and the surface regression of the ignited grains, the porosity will change with time along the bed. One typical result is shown in Fig. 10, for a shorter bed length of 8 in and an initial porosity of $\phi = 0{\cdot}47$. At the front face ($x = 0$) because of burning the solids fraction is reduced and ϕ increases with time. Two inches from that end the porosity first decreases because of bed compaction, and then after ignition at that location, ϕ increases. More severe compaction occurs at $x = 4$ but again because of grain burning the solid fraction decreases (and ϕ increases).

Based on the preliminary analysis presented in this section, it is difficult to select any single parameter as *the* most important or most sensitive. It is, however, safe to group the parameters into essentially three groups. The first group of parameters contains all of the propellant properties. Included in this group are: (a) the energy release rate, (b) burning rate constants, (c) burning rate index, and (d) the grain geometry. As might reasonably be expected, this is the most important group of parameters in the problem. The propellant characteristics must be known, and they must be known accurately. Fortunately, most of the parameters can be measured by fairly standard experimental methods.

The second parameter grouping could be labeled the interaction parameters. The explicit appearance of drag and heat-transfer coefficients in the model characterize this grouping. It is in this category that very little useful or applicable data is available. None of the available heat-transfer or drag correlations apply. This is one area where completely new experiments are required. The experiments could be difficult to design, perform, and analyze. However, before any one model can be judged as best, such an experiment must be available.

The third group might be called the sub-model group. There are two main components, both connected with the physics of the problem. Firstly, how can the effect of the primer be adequately modeled? Secondly, what is the proper boundary condition to impose on the solid phase at a moving boundary? In both of these questions there is some evidence to indicate nonlinear material behavior. For instance, primer blast waves have been observed to compact the breech end of the propellant bed. Similarly, Soper's [21] experiments clearly indicated propellant compaction at the projectile end of the bed. It appears that a continuing theoretical analysis of these modeling problems might be most fruitful.

4. CONCLUDING REMARKS

It is evident that the practical application of the numerical codes developed in this and similar programs will not occur in the very near future. Too many of the input parameters are not known accurately, and almost any code can be tailored to match any single experiment. Hence, future theoretical and experimental work should be directed at removing as much of the empiricism as possible. The specific recommendations discussed here detail the type of data that should be generated in order to aid in this process.

If at all possible, at least two types of experimental data should be taken in each experiment. Pressure measurements in guns are current state of the art. It would be appropriate to have pressure and at least one of the following: (a) gas temperature, (b) gas velocity, (c) particle velocity, and/or (d) void fraction. An experiment such as this would be very useful, even if the experiment conditions did not precisely duplicate the gun environment.

The data base concerned with heat-transfer and pressure correlations is virtually non-existent. A well conceived set of basic experiments would be most useful. Again, it is difficult to measure heat-transfer and drag coefficients in combusting beds. Some simplified, carefully modeled, laboratory scale experiments might be adequate. Data is needed throughout the packed, fluidized and bulk transport regimes.

At least three phenomena are not adequately understood and should be explored experimentally. (a) The effect of the primer blast wave is imperfectly understood. It would be very useful to be able to relate the primer design to any initial compaction which occurs in the propellant bed. (b) Stress propagation in the propellant bed should be explored. If such stress propagation is important, its characteristics should be known. (c) The impaction of the propellant on the projectile base should be studied. It is not clear if the propellant impacts and adheres to the projectile base, at least for large grains with moderate loading densities of the cartridge. These experiments are necessary before a more complete model can be advanced.

In the light of these recommendations, are the current experimental and theoretical efforts useful? The answer is yes. The experiments are slowly refining our knowledge of the physics involved and delineating important problem areas. The modeling efforts are useful in two ways. Firstly, parametric sensitivity studies can be done to identify which empirical parameters are most important. This, in turn, can be used to develop new and appropriate experimental programs. Secondly, most of the studies are being extended to handle the axisymmetric problem. When this is complete, then more realistic geometric models will be available. Such models may prove to be useful, in at least a qualitative sense, in developing scaling relations and in determining primer geometry.

Acknowledgement—The authors would like to acknowledge the assistance of Dr. S. Rajan, Research Associate, AAE Department, with the numerical solution procedures. The work was supported by the Ballistic Research Laboratories, APG, MD, under contract DAAD-05-72-C-0415.

REFERENCES

1. K. K. Kuo, Theory of flame front propagation in porous propellant charges under confinement, Ph.D. dissertation, Princeton University (August 1971).
2. K. K. Kuo, R. Vichnevetsky and M. Summerfield, Theory of flame front propagation in porous propellant charges under confinement, *AIAA Jl* **11**, 444 (April 1973).
3. K. K. Kuo and M. Summerfield, Theory of steady-state burning of porous propellants by means of a gas-penetrative mechanism, *AIAA Jl* **12**, 49–56 (January 1974).
4. H. Krier, W. Van Tassell, S. Rajan and J. VerShaw, Model of gun propellant flame spreading and combustion, in *Proceedings of the 10th JANNAF Combustion Meeting*, CPIA Publication 243, Vol. 2, 43–60. Newport, RI (December 1973).
5. M. J. Beran, *Statistical Continuum Theories*. Interscience, New York (1968).
6. Yu. A. Buyevich, Statistical hydromechanics of disperse systems, Part 1. Physical background and general equations, *J. Fluid Mech.* **49**(3), 489 (1971).
7. Yu. A. Buyevich, Statistical hydromechanics of disperse systems, Part 2. Solution of the kinetic equation for suspended particles, *J. Fluid Mech.* **52**(2), 345 (1972).
8. Yu. A. Buyevich, Statistical hydromechanics of disperse systems, Part 2. Pseudo-turbulent structure of homogeneous suspensions, *J. Fluid Mech.* **56**(2), 313 (1972).
9. T. B. Anderson and R. Jackson, A fluid mechanical description of fluidized beds—equations of motion, *I/EC Fundamentals* **6**, 527 (November 1967).
10. S. Whitaker, The transport equations for multi-phase systems, *J. Engng Sci.* **28**, 139–147 (1973).
11. P. S. Gough and F. J. Zwarts, Theoretical model for ignition of gun propellant, Report SRC-R-67, Final Report, Part II, Space Research Corporation, North Troy, Vermont (December 1972).
12. P. S. Gough and F. J. Zwarts, Private communication.
13. E. B. Fisher and A. P. Trippe, Development of a basis for acceptance of continuously produced propellant, CALspan Report No. VQ-5163-D-1 (November 1973).
14. D. R. McClure and J. L. East, Jr., Experimental techniques for investigating the start-up ignition/combustion transients in full-scale charge assemblies, in *Proceedings of the 11th JANNAF Combustion Meeting*, Vol. 1, pp. 119–139. CPIA Publication 261, Newport, RI (December 1974).
15. C. Truesdell and R. A. Toupin, The classical field theories, in *Handbuck der Physik*, Vol. III, Part 1, edited by S. Flügge, Springer, Berlin (1960). [Particular sections of interest are S. 158, p. 469—Kinematics of diffusion in a heterogeneous mixture; S. 159, p. 472—Conservation of mass in a heterogeneous mixture; S. 215, p. 567—Partial stress in a heterogeneous mixture; S. 243, p. 612—Balance of energy in a heterogeneous mixture; S. 254, p. 634—Heterogeneous media, I. Compatibility of an equation of state for the mixture with equations of state for the constituents; S. 255, p. 636—Heterogeneous media, II. Explicit form of the Gibbs Equation.]
16. C. Truesdell, *Rational Thermodynamics*. McGraw-Hill, New York (1969). [In particular, Chapter 5, Thermodynamics of diffusion, pp. 81–98.]
17. P. D. Kelly, A reacting continuum, *Int. J. Engng Sci.* **2**, 129 (May 1964).
18. S. L. Soo, *Fluid Dynamics of Multiphase Systems*. Blaisdell, Waltham, Mass. (1967).
19. S. Ergun, Fluid flow through packed columns, *Chem. Engng Prog.* **48**, 89 (1952).
20. N. I. Gelperin and V. G. Einstein, Heat transfer in fluidized beds, *Fluidization*, edited by J. F. Davidson and D. Harrison. Academic Press, New York (1971).
21. W. G. Soper, Ignition waves in gun chambers, *Combust. Flame* **20**, 157 (April 1973).

COMBUSTION ET PHENOMENE DE PROPAGATION DES FLAMMES DANS LES MATERIAUX EXPLOSIFS PERMEABLES AUX GAZ

Résumé—On analyse dans l'article la combustion et la propagation des flammes, dans des lits perméables aux gaz, de grains de combustible solide. Un modèle théorique basé sur les concepts de la mécanique des milieux continus est d'abord formulé. La méthode aux différences finies de Lax–Wendroff est alors utilisée pour obtenir des solutions numériques. La sensibilité du modèle aux caractéristiques du combustible, aux lois de transfert de chaleur et de frottement et à la densité du lit combustible est établie à l'aide des résultats numériques. On en déduit que les propriétés du combustible, et particulièrement la vitesse de libération d'énergie et l'indice du taux de combustion, sont les paramètres déterminants dans ce problème. On relève aussi l'insuffisance de lois de corrélation adaptées au problème du transfert de chaleur et du frottement dans les écoulements réactifs.

VERBRENNUNGS- UND FLAMMENAUSBREITUNGSERSCHEINUNGEN IN GASDURCHLÄSSIGEN, EXPLOSIVEN MATERIALEN

Zusammenfassung—Die Ausbreitung von Verbrennung und Flammen in gasdurchlässigen Festbetten aus festen, körnigen Treibstoffen wird in diesem Aufsatz analysiert. Ein auf dem Konzept der Kontinuumsmechanik basierendes theoretisches Modell wird zunächst aufgestellt. Die Lax–Wendroff-methode der finiten Differenzen wird dann benutzt, um einige numerische Lösungen zu erzeugen. Die Empfindlichkeit des Modells in Bezug auf Treibstoffeigenschaften, Korrelationen für Wärmeübergang und Strömungswiderstand sowie die Packungsdichte des Festbetts wird durch die numerischen Ergebnisse nachgewiesen. Es wird daraus geschlossen, daß die Treibstoffeigenschaften, insbesondere die Geschwindigkeit der Energiefreisetzung und die Maßzahl der Verbrennungsrate, die kritischsten Parameter bei diesem Problem sind. Der Mangel an geeigneten Korrelationen für Wärmeübergang und Strömungswiderstand bei Strömungen mit chemischer Reaktion wird ebenso festgestellt.

ЯВЛЕНИЯ ПЕРЕНОСА И РАСПРОСТРАНЕНИЯ ПЛАМЕНИ В ГАЗОПРОНИЦАЕМЫХ ВЗРЫВЧАТЫХ ВЕЩЕСТВАХ

Аннотация — В статье представлены результаты анализа горения и распространение пламени в газопроницаемых слоях зернистого твердого ракетного топлива. Вначале сформулирована теоретическая модель, основанная на положениях механически сплошных сред, затем с помощью метода конечных разностей Лакса–Вендроффа выполнены некоторые численные решения. На основе полученных численных результатов установлено, насколько точно модель описывает характеристики топлива, получены корреляционные соотношения по теплообмену и сопротивлению и определена плотность упаковки слоя топлива. Сделан вывод, что характеристики топлива, в особенности скорость освобождения энергии и скорость горения, являются самыми решающими параметрами в этой проблеме. Отмечен также недостаток адекватных корреляционных соотношений по теплообмену и сопротивлению для реактивных потоков.